Evaluation of the Service Life Ratio of Geogrid-Reinforced Flexible Pavement Based on Rutting and Fatigue Criteria

Aanchal Tiwari[1]*, Padma Bahadur Shahi[2], Rajan Suwal[2], Prabhat Kumar Jha[3], Ram Chandra Tiwari[2]
[1]Student, M.Sc. in Transportation Engineering, Department of Civil Engineering, Pulchowk Campus, Institute of engineering, Tribhuvan University, Lalitpur, Nepal
[2]Faculty, Department of Civil Engineering, Pulchowk Campus, Institute of engineering, Tribhuvan University, Lalitpur, Nepal
[3]Department of Road, Physical Infrastructure and Transport (MoPIT), Government of Nepal
*079mstre001.aanchal@pcampus.edu.np
(Manuscript Received 28th April, 2025; Revised 16th May, 2025; Accepted 20th May, 2025)

Abstract

This study evaluates the Service Life Ratio (SLR) of geogrid-reinforced pavement based on rutting and fatigue criteria, focusing on the Arughat–Okhale Road section of the Mid-Hill Highway in Nepal. Two demonstration sites were established at chainages 1+700m and 1+800m from the Budigandaki Bridge, located at the Dhading–Gorkha district border. The first site consists of a pavement structure without geogrid reinforcement, while the second includes a geogrid placed at the mid-base thickness of the pavement. To assess the performance and effectiveness of the geogrid reinforcement, earth pressure cells, strain gauges, and moisture sensors were installed at the mid-base level, and data were collected regularly over time. The evaluation considers an Equivalent Standard Axle Load (ESAL) of 80 kN for single axle loading. Numerical analysis using 3D finite element modeling in PLAXIS was conducted to assess pavement responses and failure mechanisms. The results indicate that for subgrade California Bearing Ratio (CBR) values ranging from 5% to 9%, rutting is the dominant failure mechanism. However, for CBR values exceeding 9%, fatigue failure becomes the governing criterion. Findings show that the inclusion of geogrid reinforcement significantly enhances pavement performance. The calculated Service Life Ratio (SLR) varies between 2.0 and 1.1 under rutting failure conditions, and between 1.0 and 1.3 under fatigue failure scenarios, depending on subgrade strength. These results suggest that geogrid reinforcement is particularly effective in weak subgrade conditions, contributing to extended pavement life and improved load distribution. This study provides valuable insights into the application of geogrids in flexible pavement design and offers guidance for prioritizing road repair and maintenance strategies.

Keywords: *Fatigue Failure, Geogrid Reinforcement, Mid-Hill Highway, Pavement Maintenance, Rutting Failure*

1. Introduction

Flexible pavements are essential components of transportation infrastructure, exposed to repetitive traffic and environmental stresses. Distresses such as rutting and fatigue significantly reduce pavement lifespan. Rutting results from permanent deformation due to traffic loads, while fatigue leads to cracking under repeated loading. Geosynthetics, especially geogrids, have been widely explored to improve pavement performance, enhance structural integrity, and extend service life.

Haas et al. (1988) first highlighted the benefits of geogrids in reinforcing granular bases, reducing rutting and enhancing pavement longevity. Geogrids redistribute traffic loads more effectively, limiting subgrade deformation and increasing durability under cyclic loading. Barksdale and Brown (1989) emphasized the role of geogrids in reducing rutting and improving structural performance. Ling and Liu (2002), using finite element analysis (FEA), confirmed that geogrid reinforcement improves resistance to both rutting and fatigue. Moayedi et al. (2009) studied geogrid effects under varying axle loads, finding improved fatigue and rutting resistance, particularly under heavy traffic.

Pandey et al. (2012) used FEA to examine geogrid placement in bituminous pavements, showing that location significantly affects fatigue and rutting strain. Their findings emphasized that proper geogrid positioning can optimize pavement behavior under both static and dynamic loads. Abu-Farsakh et al. (2014) confirmed the benefits of geogrids in reducing rutting and fatigue under cyclic loading. Banerjee et al. (2022) used PLAXIS 2D to evaluate geogrid performance under varying subgrade CBRs

and traffic, introducing a Modulus Improvement Factor (MIF) to guide design decisions. Wang et al. (2023) found that glass fiber geogrids, especially the "Grid10" type, significantly enhanced rutting resistance, extending service life. They also proposed a new flow number method for predicting rutting behavior under cyclic loads.

Despite extensive research, limited work explores how geogrid reinforcement interacts with varying subgrade CBRs in terms of both rutting and fatigue. This study aims to evaluate the service life ratio of geogrid-reinforced pavements across different subgrade CBR values using 3D computational modeling to identify dominant failure mechanisms and inform optimized pavement design strategies.

2. Materials and Methods

2.1 Study Area

The study was conducted along the Arughat-Okhale Road in the Gorkha district of Nepal, as part of the Mid-Hill Road Project. This road runs in an east-west direction, with the Budhigandaki Bridge at CH 0+000m marking the Gorkha-Dhading border. Site maps for the Gorkha District and the test locations—CH 1+700m (without geogrid) and CH 1+800m (with geogrid)—are shown in Fig.s 1 and 2.

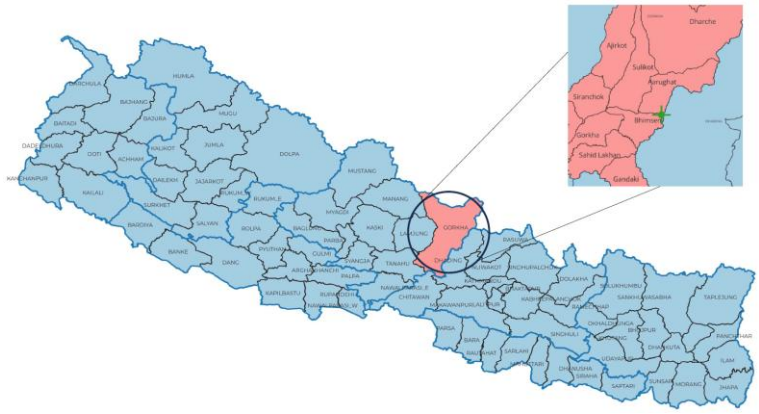

Fig. 1. Test Site Locations, Gorkha, Nepal

These sites were strategically selected as part of Nepal's national pride project, allowing for evaluation during both the construction phase and after the pavement was opened to traffic. This approach provides valuable insights into the pavement's long-term durability and real-world performance.

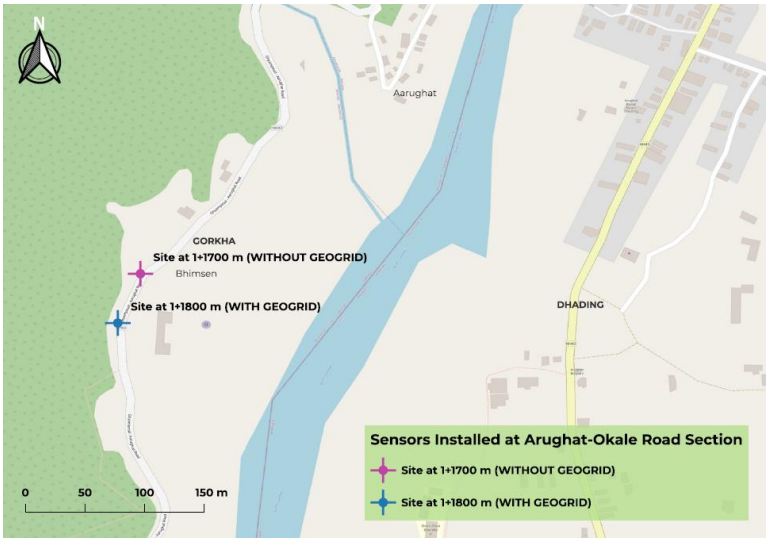

Fig. 2. Test sites at CH 1+700 m (without geogrid) and CH 1+800 m (with geogrid) along the Arughat–Okhale section of the Mid-Hill Highway

Sensors were placed beneath the geogrid at the base layer to monitor stress-strain data during

vehicle passage, with geodynamic data loggers capturing real-time pavement behavior (Fig. 3). Dynamic Cone Penetrometer (DCPT) tests were also conducted on each layer to determine field CBR values, assessing the pavement's strength and load-bearing capacity.

Fig. 3. Placement of Geogrid and Sensors: Left Fig.-40/40Q Biaxial Polypropylene Geogrid (Tensar); Right Fig.-Sensors beneath Geogrid at Mid–Depth of Base Course

2.2 Numerical Model

The geometrical model for the Arughat-Okhale section is shown in Fig. 4, representing the scaled dimensions of the pavement structure. The vehicle load configuration, as per IRC: 37-2018 (Indian Roads Congress guidelines), is depicted in Fig. 5, which uses an Equivalent Standard Axle Load (ESAL) of 80 kN per axle. This configuration is used to estimate the rutting and fatigue life of the pavement and the corresponding service life ratio, in accordance with IRC-37-2018 guidelines. Tables 1 and 2 respectively present the material properties used for linear elastic modeling of the pavement layers and the geogrid reinforcement.

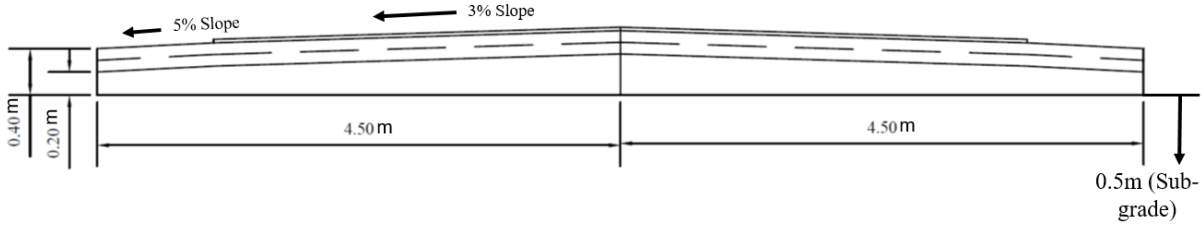

Fig. 4. Geometrical Model of Pavement

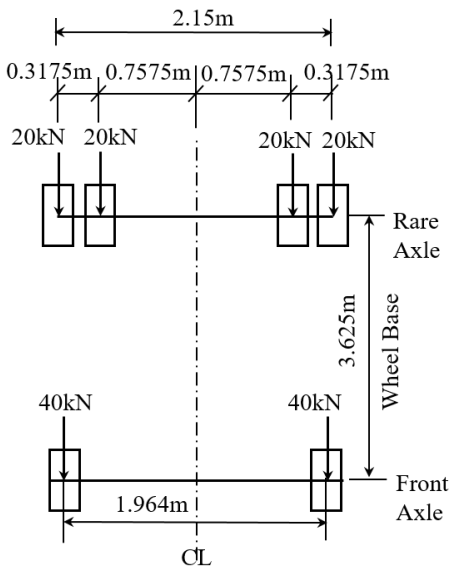

Fig. 5. Equivalent Standard Axle Load (ESAL)

Table 1 Material Models for Pavement Structure

Item	Description
Identification	Subgrade
Material model	Linear elastic
Drainage type	Undrained
Unsaturated unit weight, γ_{unsat} (kN/m^3)	18
Saturated unit weight, γ_{sat} (kN/m^3)	20
Resilient modulus, E (MPa)	E = 10.0 * CBR for CBR ≤ 5 % & E = 17.6 * (CBR)$^{0.64}$ for CBR > 5 % (FPDG, 2014) Where, E = Resilient modulus of subgrade soil CBR = California bearing ratio of subgrade soil (%)- 5%
Poisson's ratio	0.35
Identification	Granular layer
Material model	Linear elastic
Drainage type	Drained
Unsaturated unit weight, γ_{unsat} (kN/m^3)	19
Saturated unit weight, γ_{sat} (kN/m^3)	21
Resilient modulus, E (MPa)	E = 0.2*(h)$^{0.45}$ * $MR_{support}$ (FPDG, 2014) Where, h = Thickness of granular layer (mm) E = Resilient modulus of the granular layer $MR_{support}$ = (effective) resilient modulus of the supporting layer (MPa)
Poisson's ratio	0.35
Identification	DBST
Material model	Linear elastic
Drainage type	Non porous
Unsaturated unit weight, γ_{unsat} (kN/m^3)	20
Saturated unit weight, γ_{sat} (kN/m^3)	-
Resilient modulus, E (MPa)	2000 (FPDG, 2014)
Poisson's ratio	0.35

Table 2. Geogrid strength properties

Item	Description
Identification	Geogrid
Material type	Elastic
Longitudinal stiffness at 2% strain longitudinal, EA1 (kN/m)	800
Transverse stiffness at 2% strain transverse, EA2 (kN/m)	800
Shear stiffness at 2% strain, GA (kN/m)	400

Fig. 6 illustrates the meshing scheme for the 6-wheel Tata Truck 1613c point load case, modeled with an Equivalent Standard Axle Load (ESAL) of 80 kN.

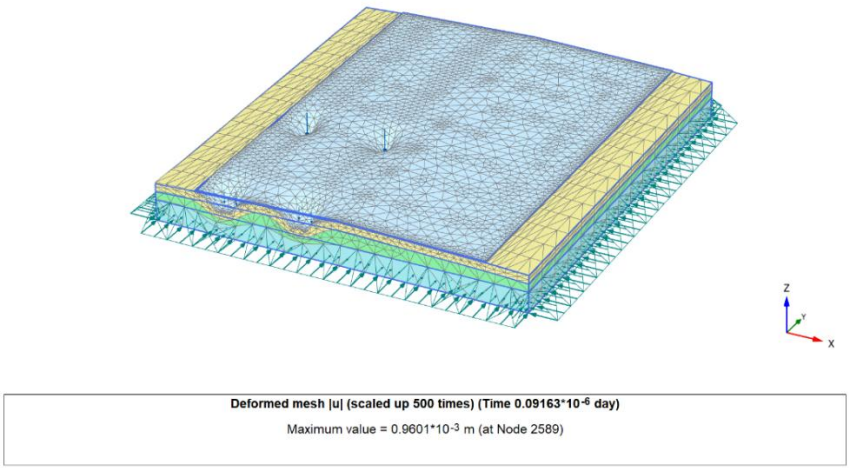

Fig. 6. Meshing Scheme of 6–Wheel Tata Truck 1613c Point Load case with ESAL of 80kN

2.2.1 Rutting and Fatigue Life of Pavement

According to IRC: 37-2018, the Rutting and Fatigue Life of pavement are two key performance criteria used in the design of flexible pavements:

- Fatigue Life refers to the number of load repetitions a pavement can withstand before cracking due to repeated tensile strain at the bottom of the bituminous layer.
- Rutting Life is based on the pavement's ability to resist permanent deformation (rutting) under compressive strain on the subgrade.

i) Subgrade Rutting Criteria for Bituminous Layer

Rutting is considered a failure when the average rut depth reaches 20 mm. Rutting life (NR) is the number of standard 80 kN axle load repetitions the pavement can withstand before reaching this limit. It is calculated using the following 1 and 2 equations.

80% Reliability:

$$N_R = 4.1656 \times 10^{-8}(1/\varepsilon_v)^{4.5337} \quad (1)$$

90% Reliability:

$$N_R = 1.4100 \times 10^{-8}(1/\varepsilon_v)^{4.5337} \quad (2)$$

Where:

N_R = Rutting life (in standard 80kN axle loads)

ε_v = Vertical compressive strain at the top of the subgrade, calculated using linear elastic layered theory

ii) Fatigue Cracking Criteria for Bituminous Layer

Fatigue failure is said to occur when 20% or more of the surface area develops interconnected cracks. The fatigue life (N_f) is the number of standard axle load repetitions until this condition is reached. The fatigue life is calculated using the following 3 and 4 equations:

80% Reliability:

$$N_f = 1.6064 \times C \times 10^{-4}(1/\varepsilon_t)^{3.89}\,(1/M_{Rm})^{0.854} \quad (3)$$

90% Reliability:

$$N_f = 0.5161 \times C \times 10^{-4}(1/\varepsilon_t)^{3.89}\,(1/M_{Rm})^{0.854} \quad (4)$$

Where:

N_f= Fatigue life (in standard 80kN axle loads)

ε_t= Horizontal tensile strain at the bottom of the bituminous layer

M_{Rm} = Resilient modulus (in MPa) of the bituminous mix

$$C = 10^M \quad (5)$$

$$M = 4.84\left(\frac{V_{be}}{V_a+V_{be}} - 0.69\right) \quad (6)$$

C = Adjustment factor accounting for the volumetric properties of the bituminous mix

V_a – Air Voids: The percentage of air spaces in the compacted bituminous mix.

Recommended Range of Design air voids: 2–2.5%

Maximum in-place air voids: Less than 4%

Low air voids help reduce moisture damage and aging. Proper compaction ensures mix durability and resistance to environmental damage.

V_{be} – Effective Bitumen Content: The percentage of bitumen that effectively coats and binds the aggregates, excluding bitumen absorbed into aggregate pores.

Recommended Range: 4–5%

2.2.2 Service Life Ratio (SLR) of Flexible Pavement

The Service Life Ratio (SLR) is a key metric used to evaluate the improvement in pavement durability achieved through reinforcement, without altering the pavement thickness. It is defined as the ratio of the vertical compressive strain at the top of the subgrade in the unreinforced condition to the corresponding strain in the reinforced condition. A higher SLR signifies enhanced durability and extended pavement life. A parametric analysis can be performed using subgrade CBR values ranging from 5% to 15% to identify the most effective conditions for pavement performance.

According to IRC:37–2018, SLR is also used to assess pavement longevity by comparing the design service life (typically 10–20 years) with the predicted life based on rutting and fatigue criteria. A higher SLR reflects a more conservative design, while a lower SLR indicates a design closer to its performance threshold. This metric assists in ensuring that the pavement structure can accommodate anticipated traffic and environmental loads, supports maintenance planning, and helps validate structural adequacy.

3. Results and Discussion

The rutting and fatigue life of the pavement have been evaluated by considering various factors and relationships as outlined in IRC: 37-2018. The results indicate a significant improvement in both rutting and fatigue strain with the inclusion of geogrid reinforcement (the unreinforced site is located at CH 1+700m, and the reinforced site at CH 1+800m). For the analysis, a rutting criterion of 20 mm was initially adopted based on linear elastic modeling using the IITPAVE software. Similarly, fatigue failure was considered to occur when 20% of the pavement area developed interconnected cracks. Both performance criteria showed noticeable improvement in strain levels with the use of geogrids. Pavement rutting and fatigue analyses were conducted and correlated with the Service Life Ratio (SLR). Pavement modeling in PLAXIS 3D was carried out based on the defined rutting and fatigue criteria.

Fig. 7 presents the typical results of strain distribution along the symmetric half-width of the road in PLAXIS 3D, considering a subgrade CBR of 5%. The top image shows the total principal strain contour, while the bottom image displays the corresponding strain plot along the section. The total maximum principal strain, as shown in Fig. 7, is 6.103×10^{-6} m, representing the maximum strain at the considered section. Input strains at the critical points—compressive strain at the top of the subgrade (for rutting analysis) and tensile strain at the base layer (for fatigue analysis)—for all CBR values (5–

15%) were determined either by identifying the corresponding node points or by extracting data from horizontal cross-sections aligned with the subgrade top and base layer coordinates, following the method illustrated in Fig. 7. Fig. 8 presents the cross-sectional strain plot corresponding to Fig. 7.

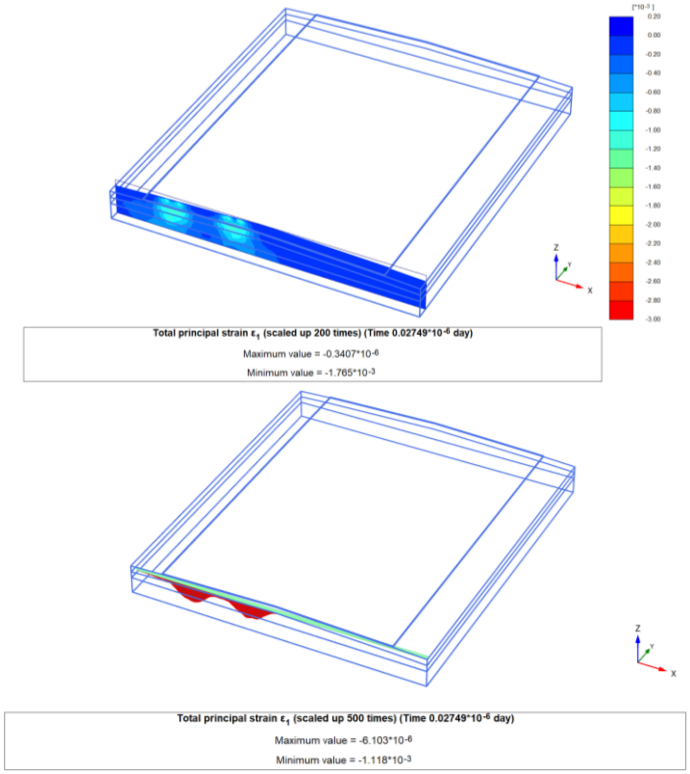

Fig. 7. Typical Results of strain plot along symmetric half-width of Road in PLAXIS 3D: Top Fig.-Total Principal strain contour; Bottom Fig.-Strain plot section

These figures represent typical outcomes of subgrade and base strain computation. After calculating the strains for subgrade CBR values ranging from 5% to 15% at both the unreinforced section (site at CH 1+700 m) and the geogrid-reinforced section (site at CH 1+800 m), the rutting and fatigue life of the pavement were further evaluated.

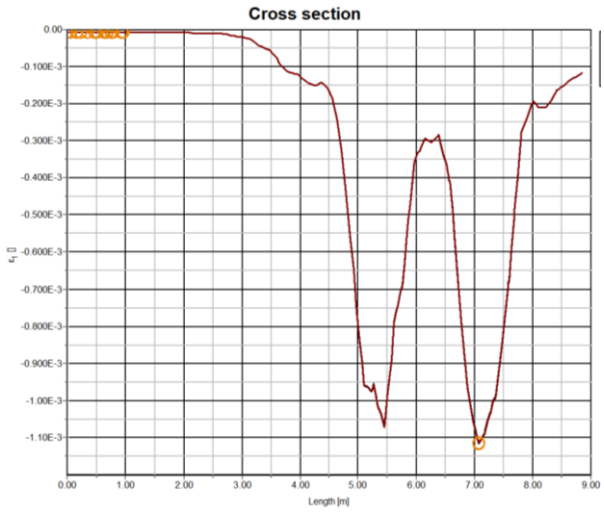

Fig. 8. Strain plot cross-section of Fig. 7

3.1 Rutting Life

Rutting is primarily a serviceability issue caused by plastic deformation in the subgrade, sub-base, or asphalt layer. For pavements designed for 5 MSA and a 10-year design life, rutting is generally expected to remain within acceptable limits (typically ≤20 mm) during the first 4–6 years, depending

on asphalt mix design, construction quality, and environmental conditions. According to IRC:37-2018, rutting failure may begin around 40–60% of the pavement life in medium MSA roads, particularly in cases of poor compaction or weak subgrade conditions (i.e., low CBR values). Fig. 9 illustrates the variation in rutting life with respect to subgrade CBR values ranging from 5–15%, for both unreinforced (site at CH 1+700m) and reinforced pavements (site at CH 1+800m). As shown in Fig. 9, rutting failure is more critical at lower CBR values. Here, "WG" represents the site without geogrid reinforcement, while "G" represents the site with geogrid.

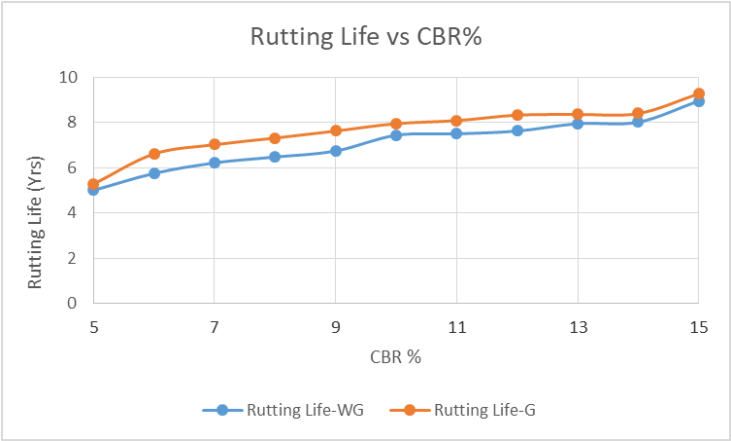

Fig. 9. Rutting Life vs. Subgrade CBR%

3.2 Fatigue Life

Fatigue cracking occurs due to repetitive tensile strain at the bottom of the asphalt layer. For a 10-year, 5 MSA design, fatigue failure typically becomes critical during years 6–10. It depends on factors such as asphalt layer thickness and annual traffic loading. The AASHTO Pavement Design Guide (1993) and IRC:37-2018 provide fatigue life equations based on tensile strain and cumulative load repetitions. The variation in fatigue life with respect to subgrade CBR values ranging from 5–15% is shown in Fig. 10, for both unreinforced (site at CH 1+700m) and reinforced pavements (site at CH 1+800m). As indicated in Fig. 10, fatigue failure tends to be more critical at higher CBR percentages. Here, "WG" represents the site without geogrid reinforcement, while "G" represents the site with geogrid.

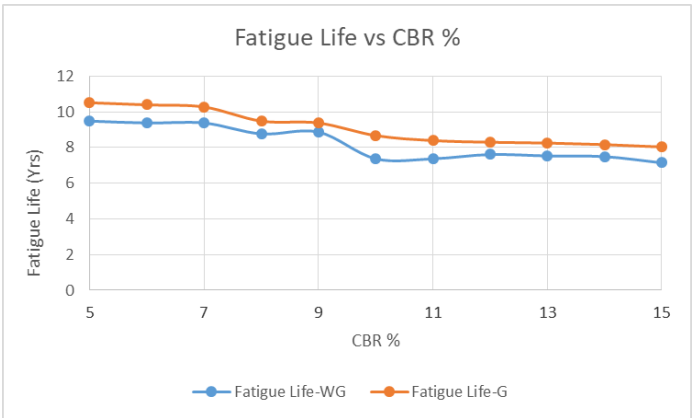

Fig. 10. Fatigue Life vs. Subgrade CBR%

The Service Life Ratio (SLR) evaluates the improvement in pavement durability by comparing performance before and after reinforcement, based on empirical relationships for rutting and fatigue failure criteria, while maintaining consistent pavement thickness. It is calculated as the ratio of vertical compressive strain at the top of the subgrade in the unreinforced state to that after reinforcement, indicating the extent of durability enhancement. Service Life Ratio (SLR) results indicated that rutting is the dominant failure mode at low CBR levels (Fig. 11), whereas fatigue becomes more critical as CBR increases (Fig. 12). These results highlight the importance of integrating geogrid reinforcement in CBR-based pavement design to achieve more durable and efficient road systems. The data used to

estimate SLR—based on rutting and fatigue criteria as shown in Fig.s 11 and 12—were obtained from the unreinforced section (site at CH 1+700m) and the reinforced section (site at CH 1+800m).

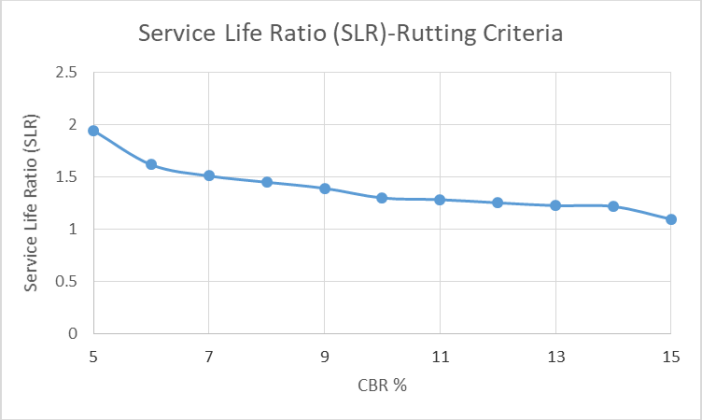

Fig. 11. SLR vs. Subgrade CBR% (Rutting Criteria)

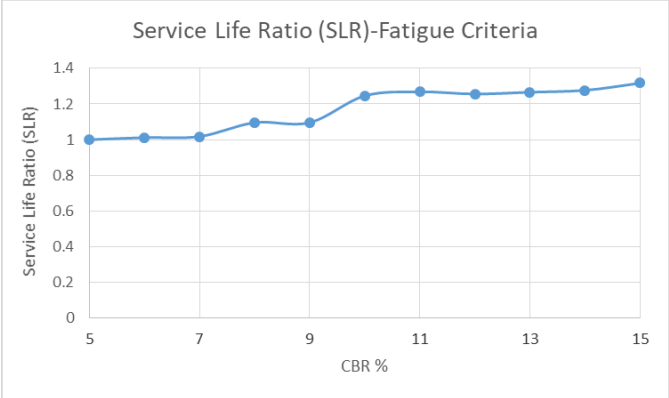

Fig. 12. SLR vs. Subgrade CBR% (Fatigue Criteria)

4. Conclusion

Geogrid reinforcement substantially improved the fatigue and rutting life of pavements, especially in subgrades with low CBR values (5–9%), where structural support is most critical. In such cases, pavement life extended by 1 to 2 years on average compared to unreinforced sections. Although benefits were also noted in higher CBR subgrades (10–15%), the gains were relatively less due to the stronger inherent support. Service Life Ratio (SLR) analysis showed that rutting failure dominates at low CBR, whereas fatigue failure becomes critical at higher CBR. These findings emphasize that CBR-based pavement design, when combined with geogrid reinforcement, leads to longer-lasting and more resilient road structures.

Acknowledgements

We would like to acknowledge the Research and Training Unit (RTU) at Pulchowk Campus and the Quality, Research and Development Center (QRDC) at the Department of Roads for supporting this research. Their contributions were essential to the success of this study, and we are grateful for their assistance.

References

Abu-Farsakh, M. Y., Gu, J., Voyiadjis, G. Z., & Chen, Q. (2014). Mechanistic–empirical analysis of the results of finite element analysis on flexible pavement with geogrid base reinforcement. International Journal of Pavement Engineering, 15(9), 786–798. https://doi.org/10.1080/10298436.2014.902516

Banerjee, S., Srivastava, V., Manna, B., & Shahu, J. (2022). A novel approach to the design of geogrid-reinforced flexible pavements. International Journal of Geosynthetics and Ground Engineering, 8, 10.1007/s40891-022-00373-3. https://doi.org/10.1007/s40891-022-003733

Barksdale, R. D., & Brown, S. F. (1989). Potential benefits of geosynthetics in flexible pavement. National Cooperative Highway Research Program. Transportation Research Board, National Research Council.

Haas, R., Walls, J., & Carroll, R. G. (1988). Geogrid reinforcement of granular bases in flexible pavements. Transportation Research Record, 1188, 19–27.

Ling, H., & Liu, Z. (2001). Performance of geosynthetic-reinforced asphalt pavements. Journal of Geotechnical and Geoenvironmental Engineering, 127(2), 177–184. https://doi.org/10.1061/(ASCE)1090-0241(2001)127:2(177)

Moayedi, H., Kazemian, S., Prasad, A., & Huat, B. K. (2009). Effect of geogrid reinforcement location in paved road improvement. Electronic Journal of Geotechnical Engineering, 14, 1–11.

Pandey, S., Rao, K. R., & Tiwari, D. (2012). Effect of geogrid reinforcement on critical responses of bituminous pavements. International Journal of Pavement Engineering, 1-17. https://doi.org/10.1080/10298436.2012.694599

Wang, S.-L., Wang, D., Tighe, S., Bhat, S., & Yin, S. (2023). Experimental study on the effects of glass fibre geogrids on rutting resistance in asphalt mixtures. Materials, 16(22), 7221. https://doi.org/10.3390/ma16227221